buildings

MDPI

Article

Integration of Photovoltaic Shading Device and Vertical Farming on School Buildings to Improving Indoor Daylight, Thermal Comfort and Energy Performance in Three Different Cities in China

Weihao Hao [1], Jiahua Xu [2], Feiyu Zhao [3], Dong-Wook Sohn [1,*] and Xuepeng Shi [4,*]

[1] The Lab of Architectural & Urban Space Design, Department of Architecture and Architectural Engineering, Yonsei University Seoul Campus, Seoul 03722, Republic of Korea; 2021313131@yonsei.ac.kr
[2] School of Design, University of Pennsylvania, Philadelphia, PA 19104, USA; jiahua@alumni.upenn.edu
[3] Department of Architecture Built Environment and Construction Engineering, Politecnico di Milano, 20133 Milano, Italy; zhaofeiyu0412@outlook.com
[4] College of Architecture and Urban Planning, Qingdao University of Technology, Qingdao 266033, China
* Correspondence: sohndw@yonsei.ac.kr (D.-W.S.); shixuepeng@qut.edu.cn (X.S.)

Abstract: This study explores the integration of photovoltaic (PV) shading devices and vertical farming (VF) in school buildings to optimize indoor daylight, thermal comfort, and energy performance across three different climate regions in China: Beijing, Shanghai, and Shenzhen. With rapid urbanization and increasing energy consumption in educational buildings, this research investigates the impact of innovative facade design on both energy efficiency and occupant comfort. Through parametric simulations and multi-objective optimization, various PV and VF facade prototypes were evaluated to determine the best configurations for reducing energy consumption while enhancing thermal and visual comfort. This study optimized facade systems integrating photovoltaic and vertical farming for school buildings in Shenzhen, Beijing, and Shanghai. Key findings include: In Shenzhen, Model B's UDI increased by 5.1% and Model C by 19.02%, with glare areas reduced by 5.4% and 21.40% and stable thermal comfort (PMV 0.52–0.59) throughout the year. In Beijing, Model B's UDI decreased by 0.2%, while Model C increased by 6.55%. Glare areas reduced by 2.92% and 14.35%, with improved winter comfort (PMV −0.35 to −0.1). In Shanghai, Model C's UDI increased by 6.7%, but summer thermal discomfort was notable (PMV up to 1.2). The study finds that PV shading systems combined with vertical farming can provide significant energy savings, reduce greenhouse gas emissions, and offer organic vegetable production within school environments. The findings suggest that integrating these systems into the building envelope can optimize the energy performance of school buildings while improving the comfort and well-being of students and staff.

Keywords: photovoltaic shading; vertical farming; thermal comfort; daylight; energy performance; school buildings

Citation: Hao, W.; Xu, J.; Zhao, F.; Sohn, D.-W.; Shi, X. Integration of Photovoltaic Shading Device and Vertical Farming on School Buildings to Improving Indoor Daylight, Thermal Comfort and Energy Performance in Three Different Cities in China. *Buildings* **2024**, *14*, 3502. https://doi.org/10.3390/buildings14113502

Academic Editor: Alessandro Prada

Received: 29 September 2024
Revised: 25 October 2024
Accepted: 29 October 2024
Published: 31 October 2024

1. Introduction

It is projected that 68% of the world's population will reside in urban areas by 2025 [1]. The accelerating process of global urbanization is expected to lead to severe energy and environmental challenges in high-density urban areas [2]. According to data from 2021, the floor area of existing school buildings in China is approximately 3.1 billion square meters, accounting for 24% of the total public building space and 50% of the common public building stock [3]. This indicates that educational buildings constitute a significant proportion of public buildings and are expanding rapidly over time. Extensive research has been conducted on comfort conditions in schools, with a primary focus on classrooms since they are crucial learning spaces where groups of people engage in educational activities for extended periods. The environment created during the learning process is considered

a factor influencing student performance and should feature motivating conditions to enhance the educational process.

In school buildings, particularly in learning spaces, proper daylight and thermal conditions are vital for facilitating the educational process, as unsatisfactory comfort levels can impair the physical and intellectual performance of teachers and students [4]. Specifically, Habibi et al. [5] highlighted that many school buildings suffer from inadequate comfort levels. Thermal conditions significantly impact occupants' health; adverse conditions can lead to apathy and even stress, affecting academic performance [6]. High temperatures can reduce work efficiency, while low temperatures decrease manual dexterity and task execution speed [7]. Summer thermal comfort is a critical factor in school building design. During summer, classrooms often do not maintain high thermal comfort levels. Due to the congregation of people, classroom temperatures usually exceed optimal levels, and the resulting stuffiness can adversely affect students' physical conditions [8]. Because schools cannot afford the high energy consumption of air conditioning, students often rely on opening windows and using fans to regulate indoor temperature and ventilation [9]. Compared to commercial buildings, school buildings typically focus on cost-effectiveness and receive less financial support. Additionally, the facade design of educational buildings, often featuring large windows, generates substantial solar gains in summer, affecting indoor thermal stability and causing thermal discomfort. In winter, regional heating systems ensure relative indoor thermal comfort but at the cost of significant energy consumption [9]. Therefore, Chinese school buildings face both thermal discomfort and excessive energy consumption.

Besides thermal discomfort, students' academic performance and teachers' health and job performance are also highly related to light comfort. Currently, the indoor illuminance and comfort levels of school buildings are still in developmental and exploratory stages. Studies have shown that daylight illumination is associated with improved mood, reduced fatigue, and decreased eye strain, and since students spend up to one-third of their day in classrooms and schools [10], classroom indoor daylight conditions are crucial. Mendell and Heath's [11] research shows that poor indoor environmental quality in schools severely impacts students' performance and attendance. Excessive contrast in lighting within students' field of view, direct sunlight exposure causing direct glare, and reflections from work surfaces and classroom blackboards causing indirect glare can all be problematic [11]. Working in environments without windows or sufficient lighting can severely disrupt the circadian system of hormone regulation [12]. Conversely, comfortable lighting strategies can alleviate student stress [13], enhancing attention and social skills [12]. Research indicates that students in classrooms with high daylight levels achieve 20% to 26% higher learning efficiency [14], underscoring the importance of optimizing shading devices in school buildings. However, fixed louvers may not meet the lighting needs of every time of day. Efficient shading systems are fundamental tasks in school renovation strategies [15]. Given the unique needs of adolescents in learning and growth, school buildings must particularly focus on indoor light comfort while minimizing energy consumption [9].

Achieving the aforementioned light and thermal comfort in classroom design is complex, as it requires balancing various interrelated factors [16]. First is the issue of energy consumption; by 2035, urbanization will lead to a 50% increase in global energy consumption compared to 1990 [17], with heating and artificial lighting in buildings accounting for 40% of global consumption [18]. In recent years, there has been an increase in reports on the environmental impact of educational buildings [19], with the average energy consumption of Chinese school buildings being 118.54 kWh/(m^2·a) [20], indicating potential for reduction. Additionally, school buildings typically have large window areas to provide natural ventilation and daylight, and the building's long axis is generally oriented east-west, with larger facade openings facing south or north, resulting in generally loose school building layouts and low energy efficiency.

Furthermore, more scholars believe that integrating food production into cities or buildings, i.e., developing urban agriculture, could alleviate the problem of food supply. There are cases showing that integrating agricultural activities in school buildings has objective social and economic value, and integrating agriculture on buildings has great potential to increase campus greening, regulate microclimates, enhance indoor comfort, reduce greenhouse gas emissions due to food transport and building energy consumption, and meet students' needs for nutrition and organic food.

Tablada and Zhao [21] and Tablada et al. [22,23] have studied the integration of solar and agricultural systems on urban and residential building facades, with Tablada proposing a simulation process for integrating building-integrated photovoltaic (BIPV) with building-integrated agriculture (BIA) on residential building facades [24]. Despite these initial studies, there is still a lack of research involving the integration of BIPV as shading devices with BIA on building facades, and research in other building types, such as schools, is very limited. Furthermore, while various methods have been proposed to optimize dynamic photovoltaic shading devices (PVSDs) [24–28], there are still research gaps: on the one hand, previous geometric optimization methods were typically based on daily experience, selecting one or a few geometric parameters for optimization, such as tilt angle and orientation [29]; currently, there is no comprehensive evaluation method to fully reveal the dynamics of PVSDs. On the other hand, there are no systematic design approaches or evaluation processes for building skin systems that integrate dynamic PVSDs and BIA. Thus, the aim of this study is to assess the feasibility of integrating BIPV with BIA on school building facades, develop and optimize a modular design framework for a building skin system that includes both dynamic PVSDs and BIA systems, considering the layout characteristics, facade features, and light and thermal environment needs of school buildings in different climate regions of China, from south to north. This aims to improve the high energy consumption, inadequate ventilation, and uneven lighting issues of school buildings, enhance visual and thermal comfort, and simultaneously provide sustainable energy and crop output. This study also contributes to positive urban environmental changes, enhances biophilic affinity, and raises awareness of the necessity to reduce greenhouse gas emissions [30], and, given that school staff and students spend a significant portion of their day at school [31] and about 30% of people [30] dine in school cafeterias, this research can shorten food miles while enabling them to access organically grown food in dense urban environments [32], positively impacting social, environmental, and economic benefits [25,33–36]. The developed architectural skin prototype relies on these features and a human-centric design philosophy to produce a synergistic effect, thus providing high-quality, sustainable solutions for retrofitting school building facades [31,37,38]. In previous studies, energy consumption control of campus buildings has generally been approached from the perspective of HVAC systems or the efficiency of energy-saving equipment and systems. Additionally, there has been relatively little research that integrates façade-based photovoltaic power generation and façade planting systems with the goal of optimizing energy efficiency in existing campus buildings while maintaining optimal indoor comfort. Some studies have achieved energy savings, but at the expense of occupant comfort. Therefore, this paper begins with the precise design variables of the building façade and the functional improvements they drive, which can significantly reduce the impact of energy optimization on occupants in existing campus buildings. From the perspective of the synergistic optimization of energy saving and comfort, the study selects the optimal façade model. Furthermore, this research conducts a comparative analysis of the relationship between variations in building façade parameters and indoor comfort levels in classrooms across different physical environments from northern to southern China.

2. Literature Review

2.1. PVSD (Photovoltaic Shading Devices)

Windows are a crucial element in buildings as they allow natural light to penetrate and provide maximum visual comfort to occupants [39]. Additionally, the ingress of natural light helps maintain the human circadian rhythm, as the body can sense light and adjust its internal biological clock, thereby regulating various bodily functions such as digestion, sleep, and mood [13,40]. However, the solar heat gains brought by sunlight are inevitable and can introduce risks of glare and overheating. When sunlight penetrates glass, it is absorbed by furniture and human bodies as short-wave radiation and then emitted as long-wave radiation, which cannot easily pass through glass, thus remaining indoors and increasing indoor temperatures [41]. Yet, Bloem et al. [42] found that shading devices can mitigate the impacts of glare [43]. External shading systems reduce the adverse effects of excessive solar penetration on the indoor light and thermal environment quality by controlling the amount of sunlight entering the interior space [44,45]. Shading systems with adjustable features can effectively control the amount of solar radiation in different seasons [42]. Proper design can prevent overheating in summer and maximize daylight ingress in winter [46]. Laura Bellia et al. proposed different types of shading approaches in their review based on the orientation and location of buildings. At the same time, studies have indicated that in the existing literature, there are few studies that have conducted a combined analysis of thermal comfort and the environment with shading devices [47].

Due to the decreasing cost of solar cells, incorporating photovoltaic energy into the building envelope has garnered significant attention [48]. Integrating photovoltaics into building roofs and facade systems is one of the holistic approaches to reducing land use. Building-integrated photovoltaics (BIPV) started in the early 1990s [17] and refer to photovoltaic components that can be integrated into the building skin (roof or facade) to meet the building's energy needs and reduce peak electrical loads. With the rise in global electricity prices and the decline in prices of photovoltaic panels, BIPV systems are becoming a cost-effective building material [49].

As a subset of BIPV, photovoltaic shading devices (PVSD) must consider the choice and efficiency of photovoltaic panel materials as well as the setting and selection of angles [50]. First, there are the photovoltaic panel materials and their power generation efficiency. Over 90% of the global photovoltaic cell market is dominated by crystalline silicon, which includes both monocrystalline and polycrystalline types. Monocrystalline silicon photovoltaic cells are especially valued for their efficiency, long-term stability, and extremely low cost. Photovoltaic cells made from monocrystalline silicon are widely used due to their high efficiency (27.6%). Besides monocrystalline silicon, thin-film photovoltaic cells (CIGS) are also common [51]. Recent data show that their efficiency is 23.4%, and they have many advantages, such as being flexible, high power, thin, and light (2.4 kg/m^2), which is beneficial for better application in facade shading panels. Secondly, the angle of the photovoltaic shading panels is critical; research shows that horizontal and vertical adjustments of shading angles can more effectively control glare [52]. Discussions on PVSD systems in terms of electrical, thermal, and lighting performance suggest that the optimal tilt angle for photovoltaic panels in Guangzhou is 30°. When setting the angles of photovoltaic panels, the geographical location's impact on the photovoltaic system should be considered [53].

2.2. Vertical Farming on Facades

Vertical farming on facades (VF) is a variant of vertical greenery systems (VGS). While much of the experience and technology from VGS are applicable to VF, they have traditionally targeted ornamental plants [54–56]. Although there is a trend towards edible plants, these are less common. Similar to rooftop agriculture compared to rooftop greening, crops may require additional systems to optimize the environmental conditions for crop growth to maximize yield per unit area, such as rooftop greenhouses [57]. The placement of agricultural systems on building facades varies according to the type of facade. Tablada

categorizes the relationship between vertical farming and facade location based on agricultural technology and facade type [58]. Growing crops in the air cavity of double-skin facades is less common and reliable than on single-skin facades. Agricultural systems on facades not only provide food to the public but also regulate indoor climate, purify air, manage urban rainwater, and alleviate human stress like conventional VGS [54–56].

The cultivation techniques applicable to VF include hydroponics, aeroponics, and aquaponics. Hydroponics involves immersing plant roots directly in a nutrient-rich liquid solution, eliminating the need for soil [59]. This method not only saves water and labor but also increases yield per unit area [60]. Aeroponics can be seen as an advancement of hydroponics because it directly sprays nutrients onto plant roots without the need for trays or containers to hold water [61]. This method can save more than 90% of water compared to traditional soil-based methods [59]. This study primarily focuses on conventional vertical farming methods, i.e., soil-based cultivation, with the impact differences from other cultivation methods still requiring further exploration.

Research on VF on facades is particularly concentrated in Singapore due to its limited arable land, heavy reliance on food imports, and urgent need for viable solutions to enhance the resilience of urban food systems against disasters [58]. Palliwal et al. found that, due to its low latitude, Singapore's buildings can receive sufficient sunlight for photovoltaic power generation and mid-level plant growth on all four cardinal directions [62]. However, more research is needed on the feasibility of facade crop cultivation in high-latitude countries. Furthermore, Tablada and Zhao [21] discovered that a plot ratio of less than 1.9, combining traditional ground-based agricultural techniques with advanced techniques such as hydroponics and A-shaped growing systems, can achieve self-sufficiency in food for residents [21]. Tablada et al. [24] designed facade systems integrating PV shading systems and lettuce pools for typical public housing buildings, including facades with public corridors, balconies, and windows [22]. This system is expected to meet 55–103% of the annual vegetable consumption of a family of four in Singapore based on facade orientation and user crop preferences. However, these yield estimates based on light calculations are imprecise and further experiments are needed to provide more reliable crop yield data. This is because the most crucial factors for normal crop growth also include temperature, water, carbon dioxide, oxygen, and nutrients [63–65]. Further exploration is needed on the feasibility of vertical farming on facades in other regions and balancing maximizing facade crop yield while accommodating user preferences.

Users can interact with and harvest crops through three methods: opening windows on the wall, using sliding rods that allow planters to move, and directly utilizing gaps in railings. However, there are public concerns about the safety of facade agriculture [66]. Although safety grills can protect crops from falling during planting and harvesting, care must be taken to maintain overall architectural aesthetics while maximizing sunlight penetration. Future research is needed on reliable, safe, and aesthetically pleasing access ways.

In terms of crop types for facades, compared to rooftop structures, facades receive less sunlight and are thus suitable for crops with low light requirements. Short plants with short growth cycles and low light requirements, such as cucumbers, tomatoes, and lettuce—especially lettuce—are considered suitable for facade cultivation [22,67]. For low-income countries like Nigeria, cultivating medicinal plants or economically valuable plants could provide additional income for residents [52]. Therefore, crop selection should consider user preferences, local weather conditions, and market demand.

Although the public is receptive to VF on facades, a survey revealed that their main concern is the price, with over 50% expressing this concern [66]. Therefore, in designing facades, it is essential to use readily available market materials, standardized designs, and other methods to reduce initial installation costs. Additionally, many studies report high maintenance costs for agricultural applications at the building level, making it necessary to adopt recycling strategies such as rainwater harvesting and solar technology (discussed in the previous section) to reduce potential maintenance costs.

2.3. Criteria for Selecting Evaluation Metrics

2.3.1. Daylight Environment Evaluation Metrics

At the early stage of architectural design, daylight factor metrics (DFMs) is a simple method that is commonly used to evaluate the interior daylighting performance under the circumstance of an overcast sky without direct sunlight [68]. However, DFMs rely on simplified assumptions and modeling to calculate daylight levels and have the disadvantage of being unable to perform dynamic analysis and assess glare; they are not as good as climate-based daylight metrics (CBDMs) in evaluating visual comfort [69]. Table 1 summarizes the main visual comfort metrics from the former literature. This paper will mainly use UDI to make a reasonable evaluation of visual comfort based on the aforementioned research results.

Table 1. Main visual comfort metrics.

	Metrics	Definition	Source
Daylight factor metrics (DFMs)	Daylight factor metrics (DFMs)	Evaluate the distribution and intensity of daylight within a space.	[68]
	Vertical daylight factor (VDF)	VDF assesses the distribution of daylight on vertical surfaces within a space	[68]
Climate-based daylight metrics (CBDMs)	Daylight autonomy (DA)	Measures the percentage of occupied hours during which a target illuminance level is met using daylight alone.	[69]
	Annual sunlight exposure (ASE)	ASE quantifies the amount of direct sunlight entering a space over a course of a year.	[69]
	Useful daylight illuminance (UDI)	UDI measures the proportion of occupied hours during which a certain target illuminance level is met.	[69]

2.3.2. Thermal Environment Evaluation Metrics

In the 1970s, Fanger proposed a classic thermal comfort evaluation formula, which includes four physical environmental factors (air temperature, radiation temperature, relative humidity, and wind speed) and two human physiological parameters (clothing thermal resistance and activity). On this basis, he developed the PMV model (predict mean votes) and the PPD index (predicted percentage of dissatisfied) to evaluate the thermal comfort index of the human body to the thermal environment and the dissatisfaction percentage of the population to the thermal environment [69]. Through the review of the latest international standards [70], American standards [71], European standards [72], and Chinese standards [52], it is found that the PMV model is widely used to evaluate the thermal comfort of the human body in a uniform and steady-state indoor environment [73]. The thermal comfort evaluation index in this paper will be calculated and analyzed based on the PMV model.

In addition to the PMV model, there is also an adaptive model developed by de Dear [21], which considers the active factors of people's physiological adaptation, psychological adaptation, and behavioral adaptation [23]. The SET* model proposed by Gagge is a two-node model based on the human body's response to the environment [17]. The multi-node model studied by Stolwijk is to simulate human thermal comfort under space conditions [74].

Jendritzky and Niibler believed that the PMV model did not correctly predict the thermal comfort in outdoor environments, and they improved and developed the Klima-Michel-Model [21]. Zhao et al. also suggested that the PMV model is not suitable for non-uniform environments, outdoor environments, and sleeping environments [75]. Wu et al. found that the adaptive model developed by de Dear was more suitable for split air-conditioned buildings with natural ventilation than the PMV model [76]. The results of

Schellen's study showed that older people's voting expectations were lower than PMV predictions because the elderly would feel hotter or colder than younger people [77]. Chaiwiwatworakul carried out an experimental comparative study on the influence of adjustable photovoltaic systems on the thermal performance of exterior wall glass windows, with the aim of enhancing indoor thermal comfort [78].

Although Fanger's PMV model has been proved to have considerable limitations, under the office building prototype in this paper, the simulated non-naturally ventilated, steady-state indoor environment for young and middle-aged people (18–60 years old), the thermal comfort evaluation index will be calculated and analyzed based on the PMV model.

2.3.3. Resource Output Evaluation Index

The biggest architectural potential for photovoltaics applied to facades is power generation. The index used to evaluate the power generation is generally kw/h, a common energy measurement unit. Wang et al. [51] compared the overall energy performance of a PV double skin façade (PV-DSF) and a PV insulating glass unit (PV-IGU), one of which was the daily power output of the two kinds of PV windows [79]. Chatzipanagi et al. investigated the monthly production capacity of BIPV using double junction amorphous silicon (a-Si) and crystalline silicon (c-Si) at 30 and 90 inclination angles [80]. Do et al. simulated the energy potential of BIPV windows and daylight-dimming systems in hot and humid climates, and they also used monthly power generation as an evaluation indicator [81]. Peng et al. studied the annual electricity production of the east, south, and west of the photovoltaic double-skin facade (PV-DSF) in a Mediterranean climate [82]. This paper will calculate the monthly production of photovoltaics from twelve months of a year.

3. Methodology

3.1. Research Framework

Figure 1 illustrates the workflow adopted in this study. The first step involves determining the typical dimensions of educational building spaces in China and constructing a representative model of such a building using Rhino modeling software (version v.7.9). The dimensions are then established. Subsequently, evaluation criteria for facade modules are defined, with power generation selected as the metric for assessing the performance of photovoltaic panels and useful daylight illuminance (UDI) as the metric for assessing the indoor light environment. The next step involves progressively determining the variable parameters of facade component design, which include the orientation of photovoltaic panel axes, the number of rows installed, their specific dimensions, the panel tilt angles, and the types of photovoltaic cells planned for use. A library of facade components is generated from various combinations of these variable elements, providing a model and theoretical basis for subsequent simulations.

Beijing, Shanghai, and Shenzhen, and extracts their corresponding weather data for subsequent simulations. The multi-objective optimization process relies on parametric modeling tools such as Rhinoceros and Grasshopper, along with performance analysis tools like Ladybug, OpenStudio, Daysim, EnergyPlus, and Radiance. Using these parametric simulation tools, programs are run n times for each facade module at 16 representative times throughout the year based on selected cities and typical educational building architectures. A multi-objective optimization process then determines the most efficient facade components for the typical educational building, identifies the optimal combination of axial directions, and generates visual heat maps describing each module combination.

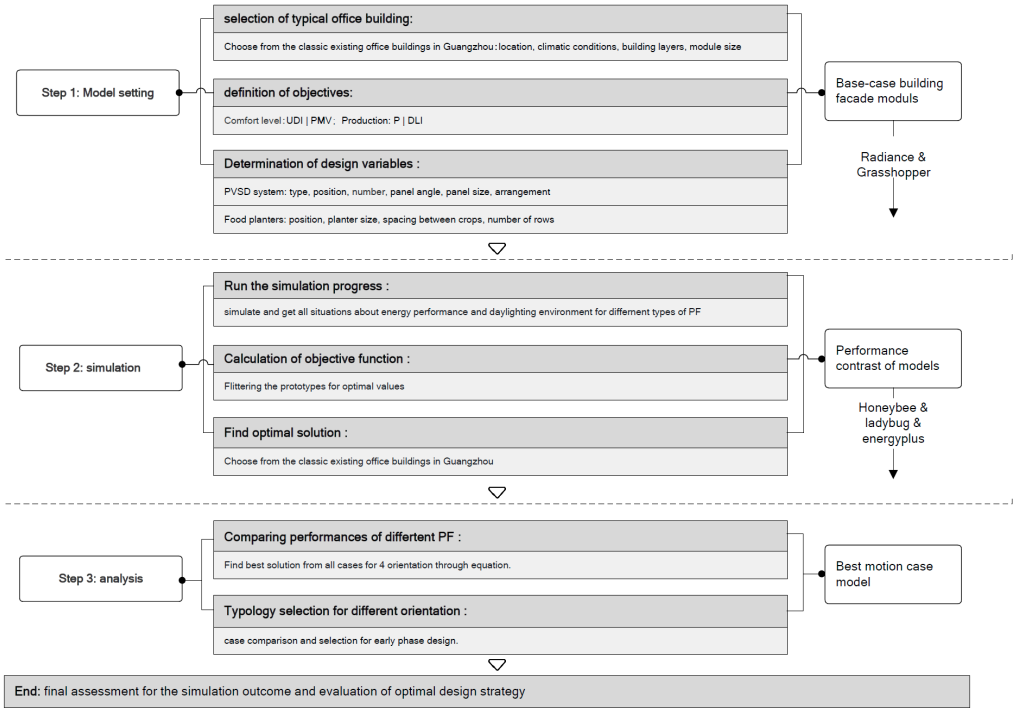

Figure 1. Framework of research method.

3.2. Selection of Typical Cities and Typical School Building Models

This research aims to explore the potential improvements to the microenvironment of school building spaces through the application of integrated VF and PV shading facade modules. Therefore, the evaluation criteria for facade modules must consider the current state of educational buildings in different cities. Due to the heat island effect brought about by rapid urban development, most campus buildings are open and well lit, prone to thermal discomfort, and also suffer from indoor glare and uneven lighting. Thus, the evaluation criteria primarily focus on the indoor thermal and light environments. From the production perspective of the facade, the power output of PV components and the crop yield from VF are also considered as evaluation metrics.

The three selected cities are Beijing, Shanghai, and Shenzhen. Beijing is located at 39.9° N latitude and 116° E longitude, with a warm temperate semi-humid semi-arid monsoon climate and an average annual temperature of 11–13 °C. Shanghai is at 31.14° N latitude and 121.29° E longitude, in the north subtropical monsoon climate zone, with distinct seasons, abundant sunlight, and plentiful rainfall. The climate in Shanghai is mild and humid, with short springs and autumns and long winters and summers, with an average temperature of 17.7 °C. Shenzhen, located between 113°46′ E to 114°37′ E longitude and 22°27′ N to 22°52′ N latitude, features a subtropical monsoon climate with long summers and short winters, a mild climate, abundant sunlight, and rainfall, with an average annual temperature of 23.3 °C.

Figure 2 displays the typical floor plans of school buildings and typical classroom spaces, simulation classroom unit dimensions, and the number of sensor points. There are two types of typical classroom building spaces, subsequently modeled in Rhinoceros for later simulations. Based on the spatial function and dimensions of facade openings, as well as differences between internal and external corridors, three categories are defined as simulation units: Model A, B, and C, representing origin classroom space, external corridors on the south side of classrooms, and internal corridors between two classrooms, respectively. This simulation primarily compares the applications of Models B and C within the actual urban climate environment, while Model A is utilized solely as a basic reference for the classroom's spatial layout. Typical classroom space features include a width of 6.6 m, a depth of 9 m, a ceiling height of 3 m, and window heights of 1.1 m and 1.2 m; both

internal and external corridor widths are 2.1 m; and 165 sensor testing points are uniformly set at a height of 0.7 m from the floor.

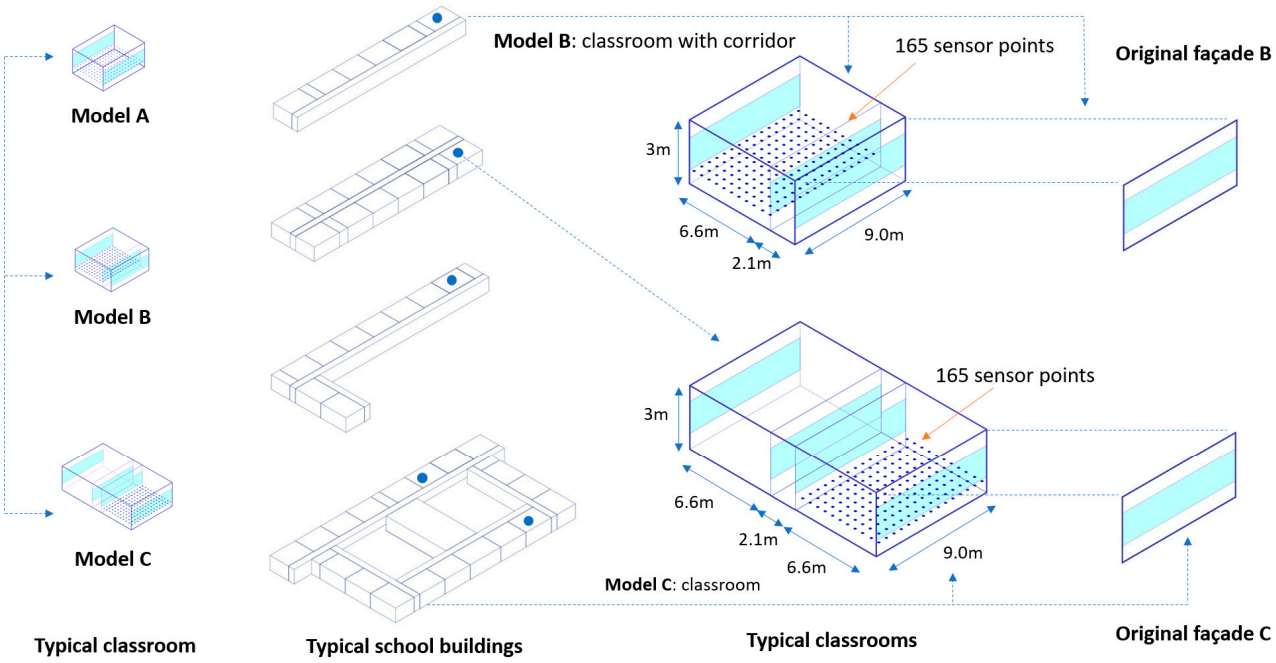

Figure 2. Research setting.

3.3. Parameter Types and Variable Settings

To integrate the advantages of PVSD and VF, the first step is to divide the facade unit vertically into three areas: upper, middle, and lower, as shown in Figure 3. Similar to the original building facade units, the upper area is primarily used for ventilation and daylighting, the middle area provides indoor daylight and a good view, and the lower area, often overlooked in the original building, serves as a wall or bay window and can be used for planting or PV. The PV shading system is suitable for the upper and middle areas, while the VF system fits better in the lower area. Since the planting system may involve drainage and irrigation facilities, it should be placed below the solar system to avoid adverse effects.

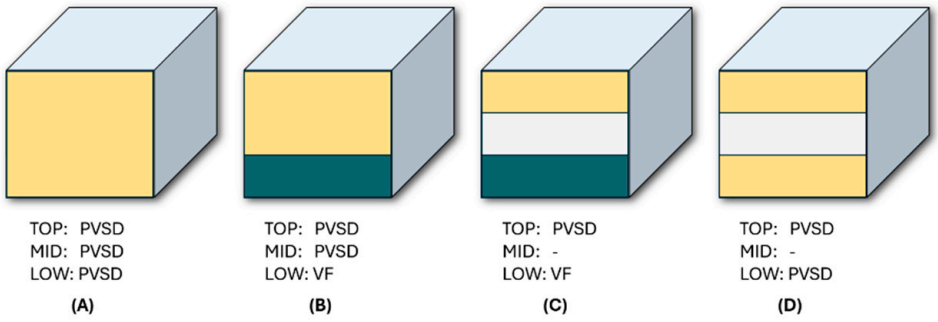

Figure 3. Prototype's vertical arrangement.

Overall design and prototype variability as shown in Figure 3, the initial partitioning possibilities of the prototype are as follows: Figure 3A Top, middle, bottom (PVSD); Figure 3B Top, middle (PVSD), bottom (VF); Figure 3C Top (PVSD), middle (none), bottom (VF); Figure 3D Top (PVSD), middle (none), bottom (PVSD).

The configuration of the photovoltaic (PV) section aims to maximize power generation while ensuring its shading function. The varying conditions of PVSD components affect the balance between renewable energy collection and improved light and thermal performance. Proper variable settings can enhance the energy performance of the components while also promoting visual comfort [83].

Photovoltaic variables include:

- PV type: Common types on the market include crystalline silicon PV and thin-film PV.
- PV panel angle: Given that an inclined PV setup can produce 20–40% more electricity than a flat vertical layout [84], angles of 20°, 30°, and 40° are chosen for the PV panels.
- PV panel layers: Options of single or double layers are considered based on size, and three arrangement modes are selected (horizontal tilt, vertical east tilt, vertical west tilt).
- PV panel size: Common sizes include 156 mm, 166 mm, 182 mm, and 210 mm [85]. Panel sizes should be multiples of solar cell sizes; therefore, the smallest solar panel unit size is set at 0.4 m × 0.4 m, with a comparison size of 0.8 m × 0.8 m.
- PV panel arrangement: Considering the operational space required for both systems on the building facade, a 0.5 m distance is maintained between the shading system and the external wall of the building.

In total, the PV shading system comprises 36 variables, including two types of cells, two panel sizes (corresponding to specific panel layers), three tilt angles, and three arrangement methods.

Variables for the VF system include:

- Crop size and row: The dimensions of the crop type planting containers must be determined based on the crop's own needs and the specifications of the building's windows. In this study, the part dimensions of the planting containers are set at 0.2 m × 0.2 m to correspond to the window size modules.
- Crop spacing: Set at 0.25 m, planting containers can be placed continuously in multiple layers along the vertical plane, with a vertical distance exceeding 400 mm to achieve maximum efficiency.

Leafy greens are often the first choice for VF due to their shallow root systems and the edibility of the entire plant [24]. Factors like water, temperature, light, and soil affect plant growth. Given Shenzhen's subtropical climate, hot and humid, the choice of vegetables is limited. Cabbage, lettuce, kale, and hydroponically grown vegetables are best suited for this climatic zone [86]. Among all these factors, light plays the most critical role in plant growth. The growth of vegetables in vertical farms is also impacted by shading from buildings, which significantly reduces light compared to traditional horizontal planting methods. Considering these constraints, prioritizing vegetables with relatively lower light requirements for facade modules is crucial. Given the high light needs of cabbage and kale [24] and the spatial constraints of vertical planting, lettuce, a shade-tolerant and smaller crop, is selected as the most suitable choice for this study.

Based on the comprehensive analysis of variable indexes of solar shading and vertical agriculture systems, 216 prototype models, including three kinds of variables, were generated. There are 24 types of photovoltaic shading systems, including 2 types of cells, 2 kinds of panel sizes (corresponding to the specific number of photovoltaic panels), 3 kinds of tilt angles, 3 kinds of arrangement modes, etc. There are two types of vertical agricultural systems (1 container size × 1 crop × 2 container layers) and five vertical zoning modes, which are combined as shown in Figure 4.

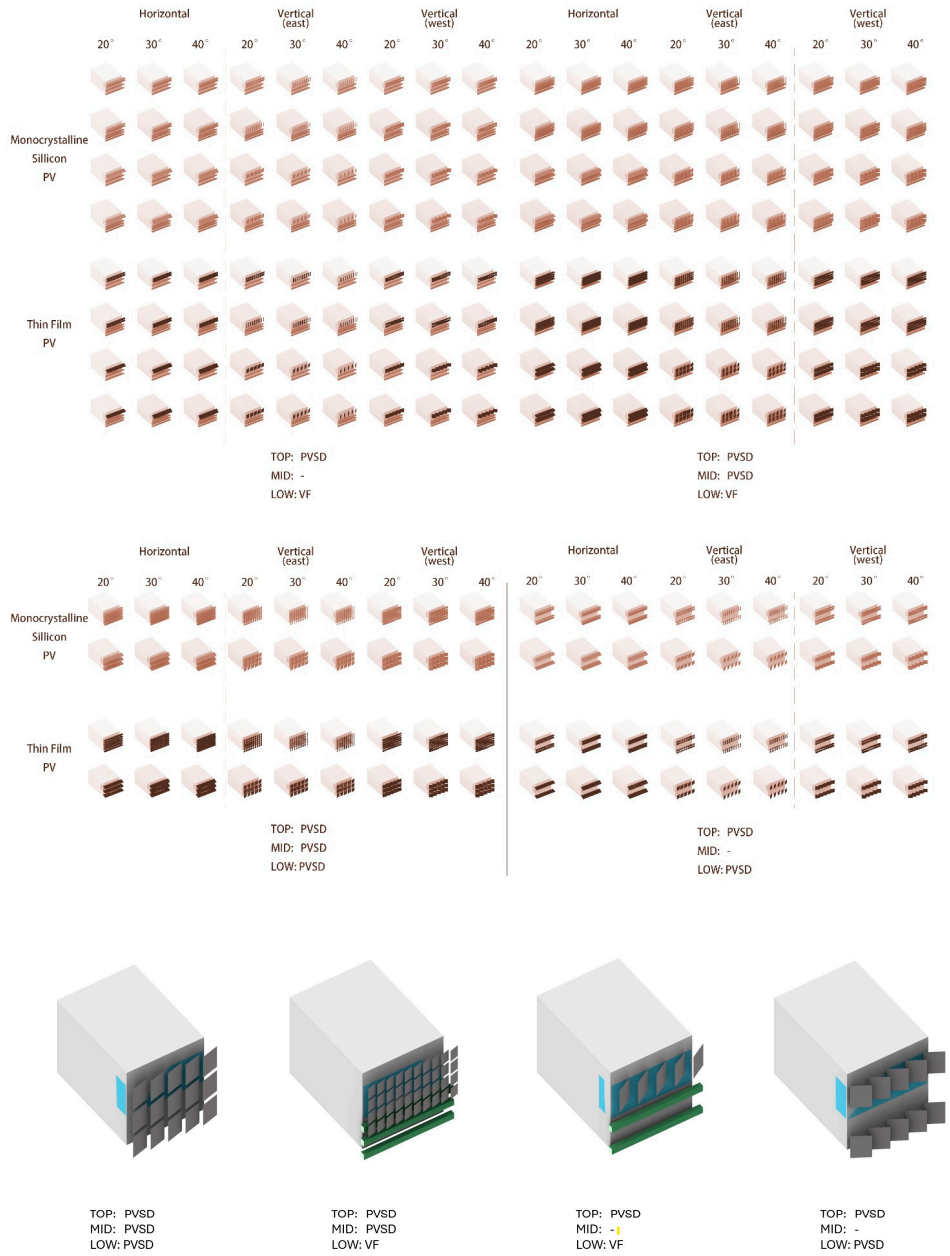

Figure 4. Prototype's resources and four typical arrangements.

3.4. Selection of Optimization Method

Regarding the selected evaluation metrics, both power generation and the impact of PVSD components on indoor daylighting and thermal environment were considered. The output power of the photovoltaics is denoted by P, representing the resource output of power generation. The evaluation indicator considered for the indoor thermal environment was the predicted mean vote (PMV), which was applied to determine appropriate options for both static and air-conditioned spaces. Visual comfort refers to the subjective perception of visual environmental comfort. Given that actual daylight levels inside buildings show significant temporal and spatial variation, the traditional concept of illuminance uniformity is insufficient to reflect real lighting conditions [87]. Therefore, a more appropriate metric for evaluating the indoor light environment is Useful Daylight Illuminance (UDI), typically ranging from 100 to 2000 lx, which is often used to calculate reasonable light distribution within buildings [87].

The optimization procedure is designed based on the multi-objective optimization method described by Equation (1) and utilizes Rhinoceros combined with the Grasshopper tool for batch processing data, extracting the optimal facade composition method.

The design prototype optimization formula (Equation (1)) is calculated as follows:

$$O_{best} = Min\left(\sqrt{\left(\left(\frac{(P_i - P_{max})}{P_{max}}\right)^2 + \left(\frac{(PMV_i - PMV_{max})}{PMV_{max}}\right)^2 + \left(\frac{(UDI_i - UDI_{max})}{UDI_{max}}\right)^2\right)}\right) \quad (1)$$

where:

UDI = average effective natural daylight illuminance (i.e., the percentage of the area with illuminance values between 200 and 3000 lx).
PMV = predicted mean vote
P = power output of the photovoltaic shading system.

The derivation of this formula: First, an ideal point for each criterion is defined, representing the best possible outcome, although it is usually unattainable. The minimum Euclidean distance formula helps find a solution close to this ideal. However, because the units of each objective function vary, the functions are transformed into dimensionless forms. Weighting is then applied to reflect the importance of each objective, with equal weight given to indoor thermal comfort, lighting, and PV power generation. The vertical farm (VF) setting, which does not affect indoor lighting, is excluded in the first optimization step. Finally, Formula (1) calculates the best-combined solution using three key indicators: power output (P), natural daylight (UDI), and thermal comfort (PMV).

The second step involves applying the component prototypes selected from the first step to their respective different city and classroom module facades, then calculating the total energy output of the photovoltaic system for the entire building facade in different cities and the total crop yield expressed as dry weight of crops [88].

3.5. Simulation Methods and Parametric Modelling

The integration of the three-dimensional modeling software Rhinoceros (version v.7.9) with the parametric programming plug-in Grasshopper facilitates the automated amalgamation and simulation of design variables for façade elements. The Ladybug [89] and Honeybee can interpret weather data via Grasshopper and utilize building performance simulation applications, including Radiance, Daysim, OpenStudio, and THERM, to analyze the data and generate visible outcomes. The Ladybug aims to do an extensive environmental analysis on a parametric platform and create interactive visualizations for visualizing meteorological data, utilizing EnergyPlus [90], Radiance [91], and Daysim [92] for daylighting and energy modeling. The meteorological data utilized for the simulation were obtained from the epwmap website.

An optimization mechanism was developed by Rhinoceros and Grasshopper to incorporate all potential prototypes consisting of variables from the VF and PVSD, resulting in 216 created design prototypes. Performance indicators were computed for each component at 16 intervals over the year. Four typical days were chosen for each season: March 22, June 22, September 22, and December 22, along with four time points for each date: 9:00 a.m., 12:00 p.m., 3:00 p.m., and 6:00 p.m. The simulations were executed independently in the virtual environments of Beijing, Shanghai, and Shenzhen, with each model comprising 3456 simulations, resulting in a total of 27,648 simulations. The simulation uses single-layer transparent glass as the glazing material. Table 2 outlines the precise specifications for various construction materials, while Table 3 summarizes the parameters for different transmissive and reflective materials.

Table 2. Characteristics of the construction materials.

Material	**Specific Heat**	**Density**	**Thickness (m)**	**Conductivity**
150 mm wall	1200	840	0.15	0.23
Material	Visible Transmittance	Solar heat gain coefficient	Thickness (m)	U-Value (W/m^2 K)
Single 6 mm glass	0.88	0.65	0.006	5.5

Table 3. Characteristics of the transmissive and reflective materials.

Material	**R Transmittance**	**G Transmittance**	**B Transmittance**	**Roughness**	**Specularity**
Glass	0.7	0.7	0.7	0.05	0
Material	R Reflectance	G Reflectance	B Reflectance	Roughness	Specularity
Wall material	0.7	0.7	0.7	0.05	0
Thin film solar cell	0	0.039	0.195	0.05	0.61
Ceiling material	0.8	0.8	0.8	0.05	0
Mono solar cell	0.3	0.3	0.3	-	-
Floor material	0.4	0.4	0.4	0.05	0
Surround building	0.2	0.2	0.2	0.05	0

4. Result

After 20,736 simulations, an optimal facade module prototype was selected for different classroom spaces in each city's educational buildings. Two best prototypes were chosen for each city, with preliminary simulations conducted only for each PV variable.

The simulation results for Model B and Model C spaces indicate that the best facade combination in any city is to have photovoltaic shading on all three sections—top, middle, and bottom—but they differ in the size of the photovoltaic panels and their angle relative to the horizontal plane. For Model B, the best prototype angle is 40° in both Beijing and Shenzhen, while it is 30° in Shanghai. For Model C, on the other hand, the best angle is 30° in both Shenzhen and Beijing, and 40° in Shanghai. Regarding the size of the photovoltaic panels, both Model B and Model C use 0.4 m in Beijing, while in Shenzhen and Shanghai, they use 0.8 m for optimal overall effects. Specific PV panel settings can be seen in Tables 4 and 5.

Table 4. Optimal results of the Model B in Beijing, Shanghai, and Shenzhen.

Region	**Panel Size**	**Interface Partition**	**Axis Direction**	**PV Type**	**VF Rows**	**Electricity Production (Annual)**
Shenzhen	0.8 M	Upper: √ Middle: √ Lower: √	40°	Monocrystalline	2	1477.18 kWh
Beijing	0.4 M	Upper: √ Middle: √ Lower: √	40°	Monocrystalline	2	1658.36 kWh
Shanghai	0.8 M	Upper: √ Middle: √ Lower: √	30°	Monocrystalline	3	1243.60 kWh

Table 5. Optimal results of the Model C in Beijing, Shanghai, and Shenzhen.

Region	Panel Size	Interface Partition	Axis Direction	PV Type	VF Rows	Electricity Production (Annual)
Shenzhen	0.8 M	Upper: √ Middle: √ Lower: √	30°	Monocrystalline	2	1505.68 kWh
Beijing	0.4 M	Upper: √ Middle: √ Lower: √	30°	Monocrystalline	2	1617.81 kWh
Shanghai	0.8 M	Upper: √ Middle: √ Lower: √	40°	Monocrystalline	0	1256.93 kWh

In Figure 5, the top left, top right, and bottom left charts respectively display the PMV variations from March 22 to December 22 at different times of the day (9 a.m., 12 p.m., 3 p.m., 6 p.m.) for the four models in Beijing, Shanghai, and Shenzhen. For either Model B or Model C, Model B (B) represents the condition before additions, i.e., Model B (before), and Model B (A) represents the condition after additions, i.e., Model B (after).

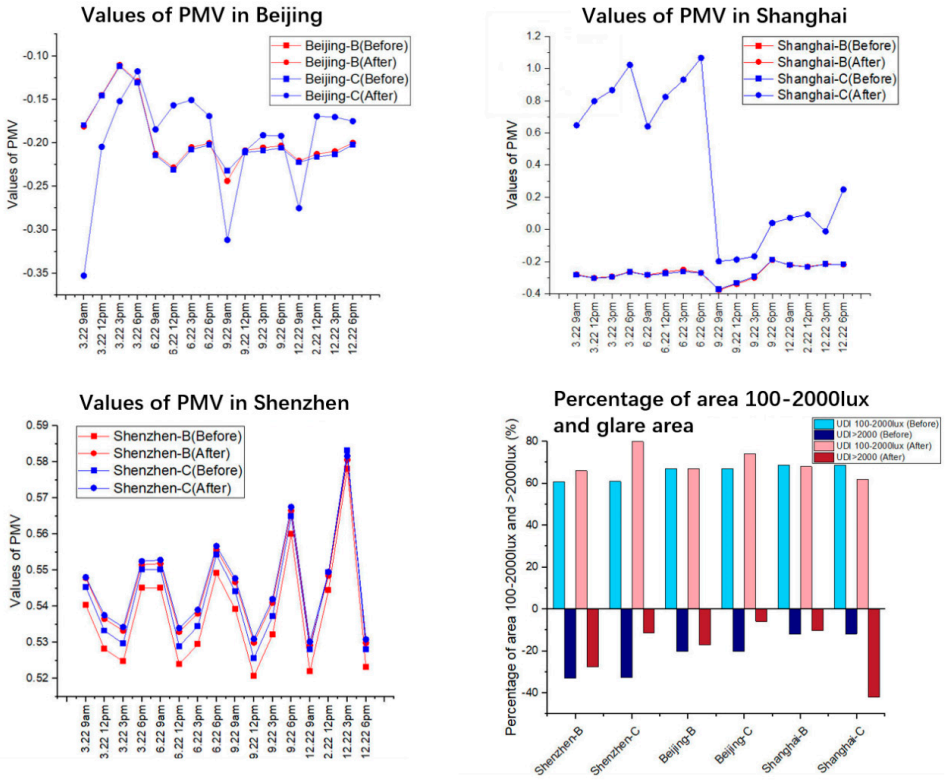

Figure 5. Diagram of PMV and UDI in three different cities.

In the top left chart, it is evident that the overall range of PMV values varies between −0.35 and −0.1, indicating a gradual decrease in PMV values over time, suggesting a gradual drop in environmental temperature. Beijing-B generally shows stable performance, with PMV closely aligned and greater PMV variation amplitude post-facade application during most time periods. After adding the facade, there are slight increases in PMV values at specific times, indicating that the application of the facade improved thermal comfort inside the classroom by reducing the sensation of cold. Comparing the initial state of Models B and C and after setting the facade, the buildings respond more distinctly to temperature changes after improvements, especially during seasonal transitions, reflecting the effectiveness of architectural environmental adjustment.

In the top right chart, compared to the situation in Beijing, Shanghai's PMV variation shows distinct differences. Firstly, the Shanghai-C (after) model shows significant PMV rises at multiple times on June 22 and September 22, with peak values approaching 1.2, indicating a very warm indoor environment at those times. Additionally, both the Shanghai-B (after) and Shanghai-B (before) models show relatively stable PMV values with small variation amplitudes, generally maintaining between -0.2 and -0.4, indicating that the building maintains good thermal comfort under these conditions. Conversely, the original Shanghai-C model shows more significant fluctuations in summer, particularly on September 22 from 6 PM to 9 PM, with PMV values sharply dropping from 1.05 to -0.4, suggesting that the weather data used for the simulation on that day may have included significant cooling. Overall, this chart effectively illustrates the response of buildings in the Shanghai area to thermal comfort under different models and seasons, particularly showing significant improvements in thermal comfort in Model C after improvements during summer, while Model B maintains consistent comfort across different seasons.

In the bottom left chart, overall, the range of PMV variation in Shenzhen is very narrow, concentrated between 0.52 and 0.59, indicating a generally consistent warm and comfortable indoor environment. Both Shenzhen-B (before) and Shenzhen-B (after) models show very small changes in PMV values, exhibiting high stability, especially between 3 pm and 6 pm on June 22 and December 22, with almost no significant changes. Shenzhen-C (before) and Shenzhen-C (after) show slightly more fluctuation, especially on September 22 and December 22, with more pronounced changes in PMV values, particularly a noticeable drop at 3 pm on December 22. Overall, the smaller changes in PMV in Shenzhen indicate that buildings in this region maintain relatively consistent thermal comfort across different seasons and times, with much smaller fluctuations compared to Beijing and Shanghai. This may reflect Shenzhen's relatively stable and comfortable climatic conditions, with building design being less sensitive to climate variability.

The bottom right chart shows the percentage of areas with UDI (useful daylight illuminance) conforming to 100–2000 lux and areas exceeding 2000 lux for visual glare in different building models before and after facade application in Shenzhen, Beijing, and Shanghai. The analysis shows that in Shenzhen, both Model B and Model C see a slight increase in the proportion of areas meeting the 100–2000 lux standard (pink bars) compared to the original models (blue bars) and a reduction in the glare zones (dark blue and dark red bars), indicating that the visual environment inside classrooms has been improved after adjustments. The data for Beijing are relatively consistent, with small improvements in models after facade application, indicating that the buildings' ability to regulate contrast is not as significant as in Shenzhen. Shanghai's situation is quite special, especially for Model C; although the 100–2000 lux area increases after facade application, the proportion of glare zones (dark red bars) significantly rises, indicating that while suitable illuminance areas have increased, it may have led to greater glare issues. Thus, the chart reflects that while daylight utilization has improved during the illuminance optimization process, it may also have brought new challenges in visual comfort in some cases, particularly evident in Shanghai's Model C.

Through the computational analysis of the power output of optimized models at different times of the day in Figure 6, it was found that the power generation trends of Model B and Model C are generally consistent. Both models exhibit lower power production in the morning, peak around noon, and then decrease, gradually dropping to zero by about 6 PM as sunlight fades. The only exception is the power generation trend in Shenzhen in March, which peaks around 3 PM, likely due to unstable weather conditions during the simulation day. A comparison of the overall power generation over several months reveals that for both Beijing and Shanghai, June features the highest power output of the year for Models B and C, with a significant gap between the best and worst months. In Shenzhen, the optimal power production occurs in September, with the poorest performance in March, but overall, due to Shenzhen's consistently ample sunlight throughout the year, the difference between the best and worst months is small. A

numerical comparison between Models B and C indicates that Model C generally performs better in Shenzhen, Model B performs better in Beijing, and there is little difference between Models B and C in Shanghai.

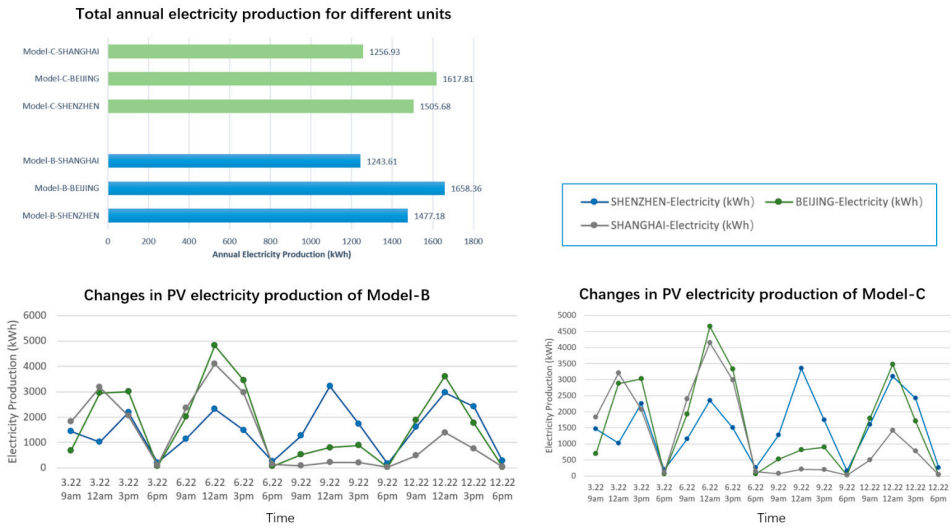

Figure 6. Diagram of electricity production in three different cities.

From the UDI heatmap in Figure 7, regardless of the region, both Model B and Model C significantly enhance indoor visual comfort, with Model C performing better. Especially in cities like Guangzhou and Shenzhen, the productive facade significantly mitigates issues of indoor glare. However, at 9 a.m. on December 22, Model B performs better than Model C. Although the changes in Shanghai and Beijing are less than those in Shenzhen, there are also clear improvements in visual comfort levels. Interestingly, in Shanghai, the indoor UDI values for Model C are nearly identical at noon and 9 a.m. on December 22, despite having significant differences initially.

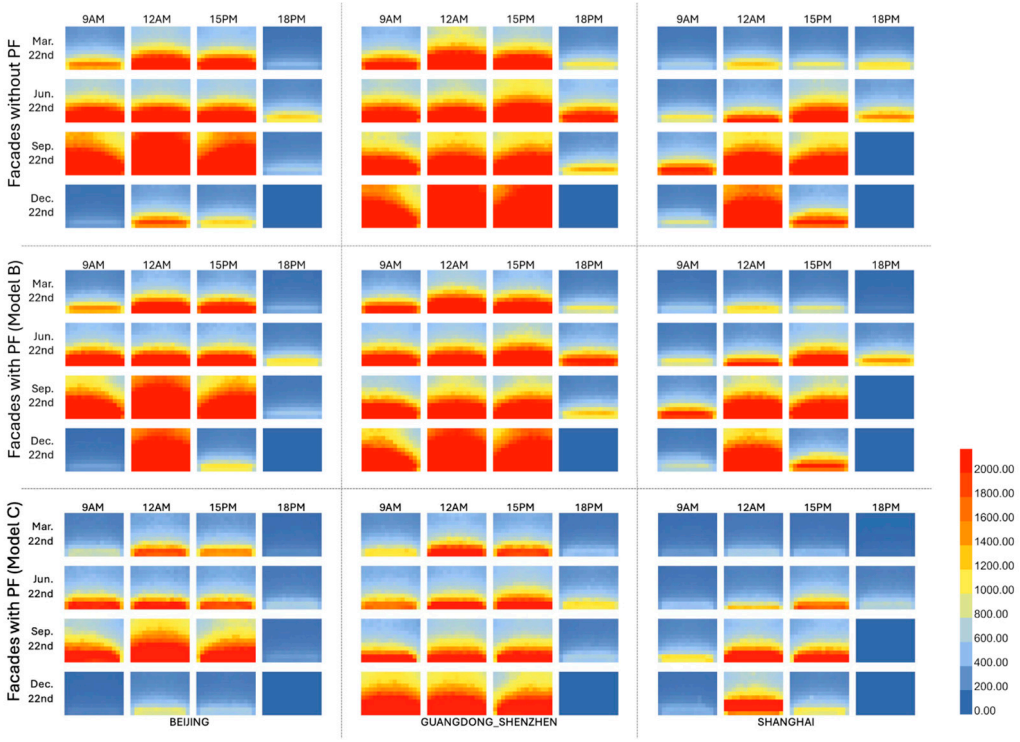

Figure 7. Diagram of UDI in three different cities.

Figure 8 illustrates vertical agriculture crop yields and average illuminance across different models and cities, highlighting the interaction between building designs and environmental variables: Both Model B and C show typical solar patterns with peak illuminance around noon, indicating effective daylight harvesting. Shenzhen exhibits delayed peak times, suggesting local environmental influences on sunlight penetration. Shenzhen achieves higher crop yields compared to Beijing and Shanghai, likely due to its favorable climate for vertical farming. Both models perform similarly within each city, suggesting that vertical farming technologies are adaptable to various architectural configurations.

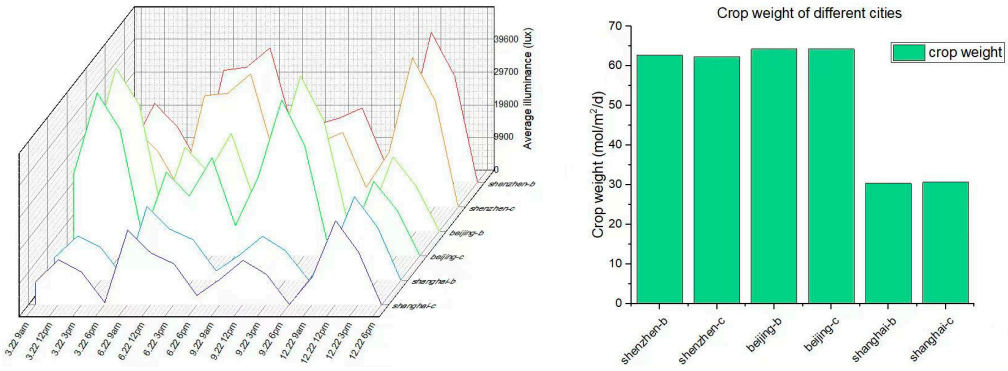

Figure 8. Diagram of vertical agriculture crop yields and average illuminance.

These insights underscore the importance of local climate in optimizing building designs for vertical farming and daylight utilization, aiding architects in enhancing sustainability in urban developments.

5. Discussion

The integration of photovoltaic shading systems and vertical farming on facades contributes to energy savings, indoor lighting, and thermal comfort in schools across three cities in China. Along with the findings from Wang et al. [52], these results demonstrate that this innovative façade system can help move China's building stock towards sustainable goals while simultaneously addressing the demand for fresh vegetables in dense urban areas.

The simulation data show that Model B exhibits smaller variations in PMV and UDI compared to Model C across the three cities, which is likely due to the presence of external corridors, differences in latitude, and varying weather conditions. These findings support previous research [21,58,62] that highlights how façade configurations, latitude, and weather conditions significantly impact sunlight availability along facades. The paper further provides evidence that the floor plans of educational buildings affect the performance of these new façade systems.

Due to the significant challenge posed by the large volume of calculations required, necessitating meticulous processing and the use of parametric tools, this study focused only on two typical educational building façade types. Nevertheless, our findings confirm the potential benefits of these innovative façade designs.

Future research should consider how to further enhance the aesthetic and customization aspects of facade module designs while achieving comprehensive indoor environmental comfort and energy efficiency. Such facade modules should not only function as practical components but also serve as significant design elements in architectural processes, crucial for reducing energy consumption in school renovation projects.

6. Conclusions

This study developed an optimization method for a productive facade unit integrating photovoltaic and agricultural systems, with a focus on both indoor and outdoor environments, particularly in school building facades. A facade model library comprising

216 samples was established by combining various design parameters related to facade component variables. Simulation programs were employed to calculate performance indices for each prototype, ultimately identifying the best-performing facade prototypes for two different classroom spaces across three cities. A multi-objective optimization method facilitated a comprehensive quantitative analysis for adaptive facade design, resource output calculations, and performance simulations. Integrating photovoltaic shading and vertical farming systems into the external walls of educational buildings can significantly enhance indoor lighting and thermal comfort in classrooms while improving the energy self-sufficiency and vegetable production capabilities of these buildings. However, the effectiveness of the facade systems in enhancing visual comfort and thermal environment varies across different cities. Quantitative analysis of optimized Models B and C in Shenzhen, Beijing, and Shanghai yields the following conclusions: In Shenzhen, Model B's useful daylight illuminance (UDI) increased by 5.1%, while Model C saw a substantial increase of 19.02%. Correspondingly, glare areas decreased by 5.4% for Model B and 21.40% for Model C. The visual comfort area increased by 12%, and glare decreased by 13.4%, with a stable PMV value ranging from 0.52 to 0.59, indicating that the indoor environment remained consistently comfortable throughout the year, with minimal seasonal impact on thermal comfort. In Beijing, Model B's UDI slightly decreased by 0.2%, whereas Model C increased by 6.55%. Glare areas decreased by 2.92% (Model B) and 14.35% (Model C). The visual comfort area improved by 4%, and glare was reduced by 8%. The PMV fluctuated between -0.35 and -0.1, indicating that the optimized facade effectively mitigated the cold sensation during winter, enhancing thermal comfort. In Shanghai, Model B's UDI decreased by 0.71%, while Model C improved by 6.7%. However, glare areas decreased 0.70% for Model C and by 7.6% for Model C, suggesting that alongside the improved daylight utilization, glare issues were also reduced. PMV values indicated discomfort during the summer months, particularly in June and September, with readings reaching 1.2, reflecting a hot indoor environment. The photovoltaic systems demonstrated varying electricity generation across cities; Beijing and Shanghai reached peak generation in June, while Shenzhen peaked in September, showing more stable annual electricity generation. Furthermore, Shenzhen's vertical agricultural yield surpassed that of Beijing and Shanghai by 18%, highlighting the effectiveness of the system in more favorable climatic conditions. Overall, these quantitative analyses underscore the significant benefits of facade systems in enhancing classroom visual comfort, reducing glare, improving thermal environments, and achieving energy self-sufficiency across varying climates. They also reveal specific challenges faced by different cities, such as glare issues in Shanghai and excessive heat during the summer.

Author Contributions: Conceptualization, W.H. and D.-W.S.; data curation, F.Z.; formal analysis, W.H.; funding acquisition, D.-W.S.; investigation, W.H.; methodology, D.-W.S. and X.S.; project administration, D.-W.S.; resources, J.X. and X.S.; software, J.X.; supervision, W.H.; validation, J.X. and F.Z.; visualization, F.Z.; writing—original draft, W.H.; writing—review and editing, J.X. and X.S. All authors have read and agreed to the published version of the manuscript.

Funding: This work was supported by the Natural Science Foundation of Shandong Province [grant numbers ZR2023QE217].

Data Availability Statement: The original contributions presented in the study are included in the article, further inquiries can be directed to the corresponding author.

Conflicts of Interest: The authors declare no conflicts of interest.

References

1. United Nations, Department of Economic and Social Affairs. 2018 Revision of World Urbanization Prospects. *Retrieved Sept.* **2018**, *18*, 2024. Available online: https://www.un.org/development/desa/en/news/population/2018-revision-of-world-urbanization-prospects.html (accessed on 1 October 2024).
2. Kim, M.; Leigh, S.-B.; Kim, T.; Cho, S. A Study on External Shading Devices for Reducing Cooling Loads and Improving Daylighting in Office Buildings. *J. Asian Archit. Build. Eng.* **2015**, *14*, 687–694. [CrossRef]

3. Peng, Z.; Yu, Y.; Guan, R. Demand-Oriented Review of a Dynamic Energy-Loss Monitoring System for Primary School Buildings through Micro-Environmental Data Monitoring and Occupant Behavior Analysis. *Buildings* **2023**, *13*, 2694. [CrossRef]
4. Ghanbaripour, A.N.; Talebian, N.; Miller, D.; Tumpa, R.J.; Zhang, W.; Golmoradi, M.; Skitmore, M. A Systematic Review of the Impact of Emerging Technologies on Student Learning, Engagement, and Employability in Built Environment Education. *Buildings* **2024**, *14*, 2769. [CrossRef]
5. Habibi, S.; Valladares, O.P.; Pena, D. New sustainability assessment model for Intelligent Façade Layers when applied to refurbish school buildings skins. *Sustain. Energy Technol. Assess* **2020**, *42*, 100839. [CrossRef]
6. Heschong, L.; Wright, R.L.; Okura, S. Daylighting Impacts on Human Performance in School. *J. Illum. Eng. Soc.* **2002**, *31*, 101–114. [CrossRef]
7. Zeiler, W.; Boxem, G. Effects of thermal activated building systems in schools on thermal comfort in winter. *Build. Environ.* **2009**, *44*, 2308–2317. [CrossRef]
8. Hänninen, O.; Haverinen-Shaugnessy, U. *School Environment: Policies and Current Status*; WHO Regional Office for Europe: Geneva, Switzerland, 2015; Available online: https://www.julkari.fi/handle/10024/126880 (accessed on 1 October 2024).
9. Zhang, A.; Bokel, R.; Van Den Dobbelsteen, A.; Sun, Y.; Huang, Q.; Zhang, Q. Optimization of thermal and daylight performance of school buildings based on a multi-objective genetic algorithm in the cold climate of China. *Energy Build.* **2017**, *139*, 371–384. [CrossRef]
10. de Dear, R.; Kim, J.; Candido, C.; Deuble, M. Adaptive thermal comfort in Australian school classrooms. *Build. Res. Inf.* **2015**, *43*, 383–398. [CrossRef]
11. Mendell, M.J.; Heath, G.A. Do indoor pollutants and thermal conditions in schools influence student performance? A critical review of the literature. *Indoor Air* **2005**, *15*, 27–52. [CrossRef]
12. Küller, R.; Lindsten, C. Health and behavior of children in classrooms with and without windows. *J. Environ. Psychol.* **1992**, *12*, 305–317. [CrossRef]
13. Edwards, L.; Torcellini, P.; Laboratory, N.R.E. *A Literature Review of the Effects of Natural Light on Building Occupants*; National Renewable Energy Lab.: Golden, CO, USA, 2002. [CrossRef]
14. Droutsa, K.G.; Kontoyiannidis, S.; Balaras, C.A.; Lykoudis, S.; Dascalaki, E.G.; Argiriou, A.A. Unveiling the existing condition and energy use in Hellenic school buildings. *Energy Build.* **2021**, *247*, 111150. [CrossRef]
15. Mohelníková, J.; Novotnỳ, M.; Mocová, P. Evaluation of school building energy performance and classroom indoor environment. *Energies* **2020**, *13*, 2489. [CrossRef]
16. Lakhdari, K.; Sriti, L.; Painter, B. Parametric optimization of daylight, thermal and energy performance of middle school classrooms, case of hot and dry regions. *Build. Environ.* **2021**, *204*, 108173. [CrossRef]
17. Ghosh, A. Potential of building integrated and attached/applied photovoltaic (BIPV/BAPV) for adaptive less energy-hungry building's skin: A comprehensive review. *J. Clean. Prod.* **2020**, *276*, 123343. [CrossRef]
18. Belussi, L.; Barozzi, B.; Bellazzi, A.; Danza, L.; Devitofrancesco, A.; Fanciulli, C.; Ghellere, M.; Guazzi, G.; Meroni, I.; Salamone, F. A review of performance of zero energy buildings and energy efficiency solutions. *J. Build. Eng.* **2019**, *25*, 100772. [CrossRef]
19. *Environment and Health EURO*. (n.d.). Available online: https://www.who.int/europe/health-topics/environmental-health (accessed on 23 August 2024).
20. Ma, H.; Du, N.; Yu, S.; Lu, W.; Zhang, Z.; Deng, N.; Li, C. Analysis of typical public building energy consumption in northern China. *Energy Build.* **2017**, *136*, 139–150. [CrossRef]
21. Tablada, A.; Zhao, X. Sunlight availability and potential food and energy self-sufficiency in tropical generic residential districts. *Sol. Energy* **2016**, *139*, 757–769. [CrossRef]
22. Tablada, A.; Chaplin, I.; Huang, H.; Kosoric, V.; Siu Kit, L.; Chao, Y.; Lau, S. Assessment of Solar and Farming Systems Integration on Tropical Building Facades. In Proceedings of the SWC2017/SHC2017, Abu Dhabi, United Arab Emirates, 29 October–2 November 2017; International Solar Energy Society: Abu Dhabi, United Arab Emirates, 2017; pp. 1–11.
23. Tablada, A.; Kosoric, V.; Lau, S.K.; Yuan, C.; Lau, S. Productive facade systems for energy and food harvesting: A prototype optimisation framework. In Proceedings of the 33rd Passive Low Energy Architecture Conference (PLEA), Edinburgh, UK, 3–5 July 2017.
24. Tablada, A.; Kosorić, V.; Huang, H.; Chaplin, I.K.; Lau, S.-K.; Yuan, C.; Lau, S.S.-Y. Design Optimization of Productive Façades: Integrating Photovoltaic and Farming Systems at the Tropical Technologies Laboratory. *Sustainability* **2018**, *10*, 3762. [CrossRef]
25. Ordenes, M.; Marinoski, D.L.; Braun, P.; Rüther, R. The impact of building-integrated photovoltaics on the energy demand of multi-family dwellings in Brazil. *Energy Build.* **2007**, *39*, 629–642. [CrossRef]
26. Li, X.; Peng, J.; Li, N.; Wu, Y.; Fang, Y.; Li, T.; Wang, M.; Wang, C. Optimal design of photovoltaic shading systems for multi-story buildings. *J. Clean. Prod.* **2019**, *220*, 1024–1038. [CrossRef]
27. Yi, H.; Kim, M.-J.; Kim, Y.; Kim, S.-S.; Lee, K.-I. Rapid Simulation of Optimally Responsive Façade during Schematic Design Phases: Use of a New Hybrid Metaheuristic Algorithm. *Sustainability* **2019**, *11*, 2681. [CrossRef]
28. Valladares-Rendón, L.G.; Schmid, G.; Lo, S.L. Review on energy savings by solar control techniques and optimal building orientation for the strategic placement of façade shading systems. *Energy Build.* **2017**, *140*, 458–479. [CrossRef]
29. Liu, J.; Bi, G.; Gao, G.; Zhao, L. Optimal design method for photovoltaic shading devices (PVSDs) by combining geometric optimization and adaptive control model. *J. Build. Eng.* **2023**, *69*, 106101. [CrossRef]

30. Vatistas, C.; Avgoustaki, D.D.; Bartzanas, T. A Systematic Literature Review on Controlled-Environment Agriculture: How Vertical Farms and Greenhouses Can Influence the Sustainability and Footprint of Urban Microclimate with Local Food Production. *Atmosphere* **2022**, *13*, 1258. [CrossRef]
31. Coma, J.; Pérez, G.; Solé, C.; Castell, A.; Cabeza, L.F. New Green Facades as Passive Systems for Energy Savings on Buildings. *Energy Procedia* **2014**, *57*, 1851–1859. [CrossRef]
32. Stec, W.J.; Van Paassen AH, C.; Maziarz, A. Modelling the double skin façade with plants. *Energy Build.* **2005**, *37*, 419–427. [CrossRef]
33. Ng, P.K.; Mithraratne, N.; Kua, H.W. Energy analysis of semi-transparent BIPV in Singapore buildings. *Energy Build.* **2013**, *66*, 274–281. [CrossRef]
34. Fath, K.; Stengel, J.; Sprenger, W.; Wilson, H.R.; Schultmann, F.; Kuhn, T.E. A method for predicting the economic potential of (building-integrated) photovoltaics in urban areas based on hourly Radiance simulations. *Sol. Energy* **2015**, *116*, 357–370. [CrossRef]
35. Freitas, S.; Catita, C.; Redweik, P.; Brito, M. Modelling solar potential in the urban environment: State-of-the-art review. *Renew. Sustain. Energy Rev.* **2015**, *41*, 915–931. [CrossRef]
36. Gautam, B.R.; Li, F.; Ru, G. Assessment of urban roof top solar photovoltaic potential to solve power shortage problem in Nepal. *Energy Build.* **2015**, *86*, 735–744. [CrossRef]
37. Wong, N.H.; Tan, A.Y.K.; Chen, Y.; Sekar, K.; Tan, P.Y.; Chan, D.; Chiang, K.; Wong, N.C. Thermal evaluation of vertical greenery systems for building walls. *Build. Environ.* **2010**, *45*, 663–672. [CrossRef]
38. Elgizawy, E.M. The Effect of Green Facades in Landscape Ecology. *Procedia Environ. Sci.* **2016**, *34*, 119–130. [CrossRef]
39. Treado, S.; Gillette, G.; Kusuda, T. Daylighting with windows, skylights, and clerestories. *Energy Build.* **1984**, *6*, 319–330. [CrossRef]
40. Aries, M.B.C. *Human Lighting Demands: Healthy Lighting in an Office Environment*; Technische Universiteit Eindhoven: Eindhoven, The Netherlands, 2005. [CrossRef]
41. Jani, D.B. Desiccant cooling as an alternative to traditional air conditioners in green cooling technology. *Instant. J. Mech. Eng.* **2011**, *1*, 1–13. [CrossRef]
42. Bloem, J.J.; Colli, A.; Strachan, P. Evaluation of PV technology implementation in the building sector. In Proceedings of the International Conference on Passive and Low Energy Cooling for the Built Environment, Santorini, Greece, 19–21 May 2005.
43. Priatman, J.; Soegihardjo, O.; Loekita, S. Towards energy efficient facade through solar-powered shading device. *Procedia-Soc. Behav. Sci.* **2015**, *179*, 266–275. [CrossRef]
44. Gago, E.J.; Muneer, T.; Knez, M.; Köster, H. Natural light controls and guides in buildings. Energy saving for electrical lighting, reduction of cooling load. *Renew. Sustain. Energy Rev.* **2015**, *41*, 1–13. [CrossRef]
45. Manzan, M.; Padovan, R. Multi-criteria energy and daylighting optimization for an office with fixed and moveable shading devices. *Adv. Build. Energy Res.* **2015**, *9*, 238–252. [CrossRef]
46. Salameh, T.; Assad, M.E.H.; Tawalbeh, M.; Ghenai, C.; Merabet, A.; Öztop, H.F. Analysis of cooling load on commercial building in UAE climate using building integrated photovoltaic façade system. *Sol. Energy* **2020**, *199*, 617–629. [CrossRef]
47. Bellia, L.; Marino, C.; Minichiello, F.; Pedace, A. An overview on solar shading systems for buildings. *Energy Procedia* **2014**, *62*, 309–317. [CrossRef]
48. Karthick, A.; Kalidasa Murugavel, K.; Kalaivani, L.; Saravana Babu, U. Performance study of building integrated photovoltaic modules. *Adv. Build. Energy Res.* **2018**, *12*, 178–194. [CrossRef]
49. Gholami, H.; Røstvik, H.N. Economic analysis of BIPV systems as a building envelope material for building skins in Europe. *Energy* **2020**, *204*, 117931. [CrossRef]
50. Alassaf, Y. Comprehensive Review of the Advancements, Benefits, Challenges, and Design Integration of Energy-Efficient Materials for Sustainable Buildings. *Buildings* **2024**, *14*, 2994. [CrossRef]
51. Hwang, T.; Kang, S.; Kim, J.T. Optimization of the building integrated photovoltaic system in office buildings—Focus on the orientation, inclined angle and installed area. *Energy Build.* **2012**, *46*, 92–104. [CrossRef]
52. Wang, Y.; Zhang, X.; Zhang, Y.; Zhang, H.; Xiong, B.; Shi, X. Multi-Objective Analysis of Visual, Thermal, and Energy Performance in Coordination with the Outdoor Thermal Environment of Productive Façades of Residential Communities in Guangzhou, China. *Buildings* **2023**, *13*, 1540. [CrossRef]
53. Konstantoglou, M.; Tsangrassoulis, A. Dynamic operation of daylighting and shading systems: A literature review. *Renew. Sustain. Energy Rev.* **2016**, *60*, 268–283. [CrossRef]
54. Bustami, R.A.; Belusko, M.; Ward, J.; Beecham, S. Vertical greenery systems: A systematic review of research trends. *Build. Environ.* **2018**, *146*, 226–237. [CrossRef]
55. Safikhani, T.; Abdullah, A.M.; Ossen, D.R.; Baharvand, M. A review of energy characteristic of vertical greenery systems. *Renew. Sustain. Energy Rev.* **2014**, *40*, 450–462. [CrossRef]
56. Douglas, A.N.; Morgan, A.L.; Rogers, E.I.; Irga, P.J.; Torpy, F.R. Evaluating and comparing the green wall retrofit suitability across major Australian cities. *J. Environ. Manag.* **2021**, *298*, 113417. [CrossRef]
57. Appolloni, E.; Orsini, F.; Specht, K.; Thomaier, S.; Sanyé-Mengual, E.; Pennisi, G.; Gianquinto, G. The global rise of urban rooftop agriculture: A review of worldwide cases. *J. Clean. Prod.* **2021**, *296*, 126556. [CrossRef]

58. Tablada, A.; Kosorić, V. Vertical farming on facades: Transforming building skins for urban food security. In *Rethinking Building Skins*; Woodhead Publishing: Sawston, UK, 2022; pp. 285–311.
59. Mir, M.S.; Naikoo, N.B.; Kanth, R.H.; Bahar, F.A.; Bhat, M.A.; Nazir, A.; Mahdi, S.S.; Amin, Z.; Singh, L.; Raja, W. Vertical farming: The future of agriculture: A review. *Pharma Innov. J.* **2022**, *11*, 1175–1195.
60. Eigenbrod, C.; Gruda, N. Urban vegetable for food security in cities. A review. *Agron. Sustain. Dev.* **2015**, *35*, 483–498. [CrossRef]
61. Eldridge, B.M.; Manzoni, L.R.; Graham, C.A.; Rodgers, B.; Farmer, J.R.; Dodd, A.N. Getting to the roots of aeroponic indoor farming. *New Phytol.* **2020**, *228*, 1183–1192. [CrossRef] [PubMed]
62. Palliwal, A.; Song, S.; Tan, H.T.W.; Biljecki, F. 3D city models for urban farming site identification in buildings. *Comput. Environ. Urban. Syst.* **2021**, *86*, 101584. [CrossRef]
63. Specht, K.; Siebert, R.; Hartmann, I.; Freisinger, U.B.; Sawicka, M.; Werner, A.; Thomaier, S.; Henckel, D.; Walk, H.; Dierich, A. Urban agriculture of the future: An overview of sustainability aspects of food production in and on buildings. *Agric. Hum. Values* **2014**, *31*, 33–51. [CrossRef]
64. Yohannes, H. A review on relationship between climate change and agriculture. *J. Earth Sci. Clim. Chang.* **2016**, *7*, 335.
65. Munoz, H.; Joseph, J. *Hydroponics: Home-Based Vegetable Production System*; Instituto Interamericano de Cooperación Para la Agricultura (IICA): Turrialba, Costa Rica, 2010.
66. Kosorić, V.; Huang, H.; Tablada, A.; Lau, S.-K.; Tan, H.T. Survey on the social acceptance of the productive façade concept integrating photovoltaic and farming systems in high-rise public housing blocks in Singapore. *Renew. Sustain. Energy Rev.* **2019**, *111*, 197–214. [CrossRef]
67. Ghazal, I.; Mansour, R.; Davidová, M. AGRI|gen: Analysis and Design of a Parametric Modular System for Vertical Urban Agriculture. *Sustainability* **2023**, *15*, 5284. [CrossRef]
68. Skarning, G.C.J.; Hviid, C.A.; Svendsen, S. The effect of dynamic solar shading on energy, daylighting and thermal comfort in a nearly zero-energy loft room in Rome and Copenhagen. *Energy Build.* **2017**, *135*, 302–311. [CrossRef]
69. Majdalani, N.; Aelenei, D.; Lopes, R.A.; Silva, C.A.S. The potential of energy flexibility of space heating and cooling in Portugal. *Util. Policy* **2020**, *66*, 101086. [CrossRef]
70. James, J.P.; Yang, X. Healthy and energy-efficient housing in hot and humid climates: A model design. *J. Harbin Inst. Technol.* **2007**, *14*, 310–313.
71. Ascione, F.; De Rossi, F.; Vanoli, G.P. Energy retrofit of historical buildings: Theoretical and experimental investigations for the modelling of reliable performance scenarios. *Energy Build.* **2011**, *43*, 1925–1936. [CrossRef]
72. Santamouris, M.; Pavlou, C.; Doukas, P.; Mihalakakou, G.; Synnefa, A.; Hatzibiros, A.; Patargias, P. Investigating and analysing the energy and environmental performance of an experimental green roof system installed in a nursery school building in Athens, Greece. *Energy* **2007**, *32*, 1781–1788. [CrossRef]
73. Sesana, M.M.; Salvalai, G.; Brutti, D.; Mandin, C.; Wei, W. ALDREN: A methodological framework to support decision-making and investments in deep energy renovation of non-residential buildings. *Buildings* **2020**, *11*, 3. [CrossRef]
74. Akbari Paydar, M. Optimum design of building integrated PV module as a movable shading device. *Sustain. Cities Soc.* **2020**, *62*, 102368. [CrossRef]
75. Krstić-Furundžić, A.; Kosić, T. Assessment of energy and environmental performance of office building models: A case study. *Energy Build.* **2016**, *115*, 11–22. [CrossRef]
76. Reddy, P.; Gupta, M.V.N.S.; Nundy, S.; Karthick, A.; Ghosh, A. Status of BIPV and BAPV System for Less Energy-Hungry Building in India—A Review. *Appl. Sci.* **2020**, *10*, 2337. [CrossRef]
77. GhaffarianHoseini, A. Intelligent Facades in Low-Energy Buildings. *Br. J. Environ. Clim. Chang.* **2013**, *2*, 437–464. [CrossRef]
78. Chaiwiwatworakul, P. Adjustable PV Slats for Energy Efficiency and Comfort Improvement of a Radiantly Cooled Office Room in Tropical Climate. *Buildings* **2024**, *14*, 3282. [CrossRef]
79. Giovannini, L.; Verso, V.R.L.; Karamata, B.; Andersen, M. Lighting and Energy Performance of an Adaptive Shading and Daylighting System for Arid Climates. *Energy Procedia* **2015**, *78*, 370–375. [CrossRef]
80. Mahmoud, A.H.A.; Elghazi, Y. Parametric-based designs for kinetic facades to optimize daylight performance: Comparing rotation and translation kinetic motion for hexagonal facade patterns. *Sol. Energy* **2016**, *126*, 111–127. [CrossRef]
81. Tabadkani, A.; Shoubi, M.V.; Soflaei, F.; Banihashemi, S. Integrated parametric design of adaptive facades for user's visual comfort. *Autom. Constr.* **2019**, *106*, 102857. [CrossRef]
82. Shi, S.; Sun, J.; Liu, M.; Chen, X.; Gao, W.; Song, Y. Energy-Saving Potential Comparison of Different Photovoltaic Integrated Shading Devices (PVSDs) for Single-Story and Multi-Story Buildings. *Energies* **2022**, *15*, 9196. [CrossRef]
83. Jeong, K.; Hong, T.; Koo, C.; Oh, J.; Lee, M.; Kim, J. A prototype design and development of the smart photovoltaic system blind considering the photovoltaic panel, tracking system, and monitoring system. *Appl. Sci.* **2017**, *7*, 1077. [CrossRef]
84. Freitas, S.; Brito, M.C. Maximizing the Solar Photovoltaic Yield in Different Building Facade Layouts. In Proceedings of the European Photovoltaic Solar Energy Conference and Exhibition, Hamburg, Germany, 14–18 September 2015; pp. 14–18.
85. Beinert, A.J.; Romer, P.; Heinrich, M.; Mittag, M.; Aktaa, J.; Neuhaus, D.H. The effect of cell and module dimensions on thermomechanical stress in PV modules. *IEEE J. Photovolt.* **2019**, *10*, 70–77. [CrossRef]
86. Bay, J.H.P.; Owen, L.C.W.; Singh, S. Food production and density: The design of a high-rise housing development in Singapore. In *Growing Compact: Urban Form, Density and Sustainability*; Bay, J.H.P., Lehmann, S., Eds.; Routledge: Abingdon, UK, 2017.

87. Dardir, M.; Berardi, U. Development of microclimate modeling for enhancing neighborhood thermal performance through urban greenery cover. *Energy Build.* **2021**, *252*, 111428. [CrossRef]
88. Kelly, N.; Choe, D.; Meng, Q.; Runkle, E.S. Promotion of lettuce growth under an increasing daily light integral depends on the combination of the photosynthetic photon flux density and photoperiod. *Sci. Hortic.* **2020**, *272*, 109565. [CrossRef]
89. Sadeghipour Roudsari, M.; Pak, M.; VIOLA, A. Ladybug: A parametric environmental plugin for grasshopper to help designers create an environmentally-conscious design. In Proceedings of the Building Simulation 2013: 13th Conference of IBPSA, Chambéry, France, 25–28 August 2013; Volume 13, pp. 3128–3135.
90. Romero, R.; Simon, J.; Ryan, T.; Peterson, Z.; Torcellini, P.; Kandt, A.; Young, M.; Rothgeb, S.; Colgan, C. *US Department of Energy Solar Decathlon Competition Guide: 2021 Design Challenge and 2023 Build Challenge (No. NREL/BK-7A40-78944)*; National Renewable Energy Lab. (NREL): Golden, CO, USA, 2021.
91. Ward, G.J. The RADIANCE lighting simulation and rendering system. In Proceedings of the 21st Annual Conference on Computer Graphics and Interactive Techniques, Orlando, FL, USA, 24–29 July 1994; pp. 459–472.
92. Reinhart, C.F.; Walkenhorst, O. Validation of dynamic RADIANCE-based daylight simulations for a test office with external blinds. *Energy Build.* **2001**, *33*, 683–697. [CrossRef]